COMPARISON OF AN OIL-BATH BLACKBODY TO A WATER-BATH BLACKBODY USING THE NIST TXR

Benjamin K. Tsai and Joseph P. Rice

National Institute of Standards and Technology, Optical Technology Division, Gaithersburg, MD, USA

ABSTRACT

A NIST-developed filter radiometer (TXR or Thermal-infrared Transfer Radiometer) was used to perform a radiometric comparison of an oil-bath blackbody (OBBB) source with a water-bath blackbody (WBBB) source. In the NIST Ambient Background Infrared Calibration Laboratory, the WBBB and OBBB sources are used for calibration of radiation thermometers at temperatures from 15 ºC to 90 ºC and from 70 ºC to 180 ºC, respectively. A direct comparison of these two sources at a wavelength of 10 μm was performed by using the TXR to measure the radiance at blackbody temperatures between 70 ºC and 90 ºC in increments of 5 ºC. Blackbody exit aperture diameters of 4 cm, 5 cm, and 10.8 cm were used. Then the TXR, calibrated between 70 ºC and 90 ºC, was used to check the OBBB in its normal operating range between 100 ºC and 160 ºC in increments of 10 ºC. Results show that the OBBB radiance temperature is systematically lower than the WBBB radiance temperature for the same contact thermometer setting. The main goal of this study was to explain the apparent discrepancies in radiance temperature between the OBBB and the WBBB.

1. INTRODUCTION

For calibration of test radiation thermometers and blackbody sources, the NIST Ambient Background Infrared Calibration Laboratory implements an array of stable and uniform standard sources for in-house research and calibration activities and for various military and industrial applications. Two of these standard sources, a water-bath blackbody (WBBB) and an oil-bath blackbody (OBBB), were developed to cover the temperature range from 15 ºC to 180 ºC. Previous measurements suggested a discrepancy between the two blackbody sources at 70 ºC. The goal of this study is to demonstrate the utility of the NIST Thermal-infrared Transfer Radiometer (TXR) in the measurement of this temperature discrepancy and to explain the discrepancy using a simplified heat-transfer model. An understanding of the temperature discrepancy between the two bath blackbody (BBB) sources will establish greater confidence in the calibration facility by strengthening the uncertainty analysis. Discussion of extending the model to include more realistic conditions and of using the TXR in future research will be given.

2. BATH BLACKBODY SOURCES

Both BBBs are constructed with a copper cavity coated with an enamel paint for emissivity enhancement and fitted with a 10.8 cm diameter aperture [1, 2]. From Monte Carlo modeling, the emissivity of the cylindrical-conical cavity is calculated to be 0.9997 ± 0.0003 ($k = 1$). The BBB temperature is measured using a standard platinum resistance thermometer (SPRT) calibrated at NIST against the 1990 International Temperature Scale.

3. TRANSFER RADIOMETER (TXR)

The TXR is a two-channel, liquid-nitrogen cooled, transportable filter radiometer. Channel 1 is centered near 4.973 μm and has a bandwidth of about 0.9 μm, while Channel 2 is centered near 10.090 μm and has a bandwidth of about 0.95 μm. In this study, we will not consider the Channel 1 data because of the water-vapor absorption issues. The TXR components are sealed off in vacuum and cooled to near 77 K. In this study, the TXR operates in the ambient mode where

the TXR cryostat case, including the ZnSe cryostat window, is near room temperature. Other details of the TXR have been described previously [3-6].

4. TEST PROCEDURES

After the TXR was properly aligned and set up, the BBB temperature was allowed to come to steady state. For data acquisition, one of two apertures, 4 cm diameter and 5 cm diameter, were installed according to the following recipe: fully open (10.8 cm diameter opening), 4 cm, fully open, 5 cm, fully open. At each aperture opening, we measured for 10 min to 15 min. This was performed for both the WBBB and the OBBB between 70 ºC and 90 ºC in increments of 5 ºC. After calibrating against the WBBB (see Figures 1, 2, and 3), the TXR measured the OBBB in its normal operating range between 100 ºC and 160 ºC in increments of 10 ºC.

5. DATA AND MODEL ANALYSIS PROCEDURES

The response [mV], $r_2(T)$, of TXR Channel 2 to the BBB, is given by the measurement equation

$$r_2(T) = \int R_{2\lambda}(\lambda) \cdot \varepsilon(\lambda) \cdot B(\lambda,T)\, d\lambda + \int R_{2\lambda}(\lambda) \cdot \left[1 - \varepsilon(\lambda)\right] \cdot B(\lambda,T_o)\, d\lambda \tag{1}$$

where T is the thermodynamic temperature [K], T_o is the ambient temperature [K], λ is the wavelength [μm], ε is the BBB emissivity hereafter approximated as a constant independent of wavelength, $R_{2\lambda}$ is the absolute spectral responsivity of TXR Channel 2, and $B(\lambda, T)$ is the spectral radiance [W/cm^2/sr/nm] from the Planck function,

$$B(\lambda,T) \equiv \frac{c_{1L}}{\lambda^5\left[\exp(c_2/(\lambda T)) - 1\right]}, \tag{2}$$

The fundamental radiation constants, c_{1L} and c_2 [7], are shown in Table 1. The function $R_{2\lambda}(\lambda)$ can be expressed in terms of an idealized box-car absolute responsivity function that has a constant magnitude of R_2 between two wavelengths, λ_{2lo} and λ_{2hi}, and is zero elsewhere. Values for R_2, λ_{2lo}, and λ_{2hi} [8] are listed in Table 1. The TXR calibration of Channel 2 is then naturally expressed in terms of the band-integrated radiance from an ideal blackbody, $L_{B2}(T)$ [W/cm^2/sr], defined as

$$L_{B2}(T) \equiv \int_{\lambda_{2lo}}^{\lambda_{2hi}} B(\lambda,T) d\lambda \tag{3}$$

Calibrated, band-integrated radiance values resulting from response measurements are defined as

$$L_{X2}(T_c) \equiv \frac{r_{X2}(T_c)}{R_2}. \tag{4}$$

where the subscript "X" denotes values from when the TXR viewed the BBB and T_c is the SPRT temperature [K] in the fluid. Calibration of the TXR in this paper was performed against the WBBB from 70 ºC to 90 ºC with all of the apertures to obtain R_2. Since R_2 is independent of temperature and aperture size, it can be used in Eq. (4) in the conversion of r_{X2} to L_{X2}.

Table 1: Calibration parameters for the TXR.

Parameter Name	Symbol	Units	Channel 2 Value
TXR Channel #	i	N/A	2
First radiation constant for spectral radiance	c_{1L}	$W \cdot m^2/sr$	$1.19104282 \times 10^{-16}$
Second radiation constant	c_2	$m \cdot K$	1.4387752×10^{-2}
TXR low wavelength band edge	λ_{2lo}	µm	9.615
TXR high wavelength band edge	λ_{2hi}	µm	10.565
TXR responsivity (from calibration with WBBB 4 cm)	R_2	$mV \cdot cm^2 \cdot sr/W$	5.64936×10^4
Combined uncertainty of R_2; Type A, k=1	$u_c(R_2)$	%	0.152
Emissivity of NIST WBBB at 4 cm	ε_2	-	0.99997
Combined uncertainty WBBB emissivity; Type B, k=1	$u_c(\varepsilon_2)$	-	0.00003
Polynomial coefficient for T_2 to L_{B2} conversion	p_{20}	-	-1.311163
Polynomial coefficient for T_2 to L_{B2} conversion	p_{21}	-	2.041074×10^{-1}
Polynomial coefficient for T_2 to L_{B2} conversion	p_{22}	-	2.166864×10^{-2}
Polynomial coefficient for T_2 to L_{B2} conversion	p_{23}	-	1.572507×10^{-3}
Polynomial coefficient for T_2 to L_{B2} conversion	p_{24}	-	4.336041×10^{-5}

The OBBB is assumed to have a band-weighted, temperature-independent emissivity ε_{X2}. The radiance measured by Channel 2 of the TXR when it views the OBBB is modeled as

$$L_{X2}(T_c) = \varepsilon_{X2} L_{B2}(T_c + \Delta T) + (1 - \varepsilon_{X2}) L_{B2}(T_o) \tag{5}$$

which is a sum of the OBBB direct emitted radiance and the background reflected radiance. A useful quantity is the difference between the measured radiance and the ideal blackbody radiance,

$$\Delta L_2(T_c) \equiv L_{X2}(T_c) - L_{B2}(T_c) \tag{6}$$

This radiance difference can also be modeled as a second-order polynomial in the form of

$$\Delta L_2(T_c) = m_{12}\left[L_{B2}(T_c) - L_{B2}(T_o)\right] + m_{22}\left[L_{B2}(T_c) - L_{B2}(T_o)\right]^2 \tag{7}$$

The best-fit values for the two fitting parameters, m_{12} and m_{22}, listed in Table 2 can be related to the model parameters by combining Eq. (5) through Eq. (7). Comparison of the T_c-independent terms gives the emissivity in terms of known quantities,

$$\varepsilon_{X2} = 1 + m_{12} - m_{22} L_{B2}(T_o) \tag{8}$$

while comparison of the T_c-dependent terms yields the implicit ΔT versus T_c function,

$$L_{B2}(T_c + \Delta T) = \frac{\left\{\varepsilon_{X2} + m_{22}\left[L_{B2}(T_c) - L_{B2}(T_o)\right]\right\} L_{B2}(T_c)}{\varepsilon_{X2}} \tag{9}$$

The quantity ΔT is the radiating copper surface temperature T_{cu} minus T_c. From Eq. (3), $L_{B2}(T)$ is a function of T. Conversely, given a value for L_{B2}, its corresponding value of T can be computed from an inverse function $T_2(L_{B2})$. For the particular values of λ_{2l}, and λ_{2hi} listed in Table 1, values of the inverse function were computed and fit by a 4th order polynomial [8], yielding the following,

$$T_2(L_{B2}) \equiv \frac{T_N}{\sum_{j=0}^{4} p_{2j} \left\{-\ln\left[L_{B2} / L_{B2}(T_N)\right]\right\}^j} \tag{10}$$

where the coefficients p_{2j} are in Table 1 and T_N = 100 K is a normalization temperature to make the p_{2j} coefficients dimensionless. Values of T_2 computed from Eq. (10) agree with corresponding values of T inserted into Eq. (3) to within ±2 mK, over the full temperature range of the fit from 283 K to 445 K, wherein the values of p_{2j} are valid. From Eqs. (9) and (10), ΔT can be written as

$$\Delta T(T_c) = \frac{T_N}{\sum_{j=0}^{4} p_{2j}\left[-\ln\frac{\{\varepsilon_{X2} + m_{22}[L_{B2}(T_c) - L_{B2}(T_o)]\}L_{B2}(T_c)}{\varepsilon_{X2}\cdot L_{B2}(T_N)}\right]^j} - T_c \,, \tag{11}$$

The ΔL_2 function plotted in Fig. 4 as the three lines is the value of the measured radiance minus the band-integrated radiance for Channel 2. Equivalently, it is also the measured OBBB radiance minus the measured WBBB radiance for Channel 2 because the WBBB was used to calibrate the TXR [9]. At the background value of 9.397128 W/m^2/sr, the ΔL_2 function passes through zero.

Table 2: Best fit parameters in the model of Eq. (6) for Channel 2.

Aperture diameter (cm)	4	5	11
Fitting parameter, m_{12}	-0.0031261	-0.0050419	-0.014754
Fitting uncertainty, dm_{12}	0.00060397	0.00051868	0.00057735
Fitting parameter, m_{22} (m^2·sr/W)	-0.0001058	-0.00010371	-0.00015944
Fitting uncertainty, dm_{22} (m^2·sr/W)	2.3865E-5	2.0495E-5	2.2813E-5
OBBB emissivity, ε_{X2}	0.99787	0.99593	0.98674
Background, $L_{B2}(T_o)$ (W/m^2·sr)	9.397128	9.397128	9.397128

6. RESULTS

TXR temperature measurements of the BBBs at 70 ºC are shown in Figures 1 and 2. BBB temperatures calculated from averages of 30 points near the stable portion of the temperature plateau were used in the calculation of ΔL in Fig. 4. Measured temperatures using the 4 cm and 5 cm apertures were greater than those using the 10.8 cm aperture because the smaller apertures enhance the blackbody emittance. The calibration parameters, ε_{X2} and R_2, calculated from the WBBB data between 70 ºC and 90 ºC were used with the OBBB data between 100 ºC and 160 ºC (such as the data at 160 ºC in Fig. 3) to produce the ΔT data of Fig. 5 above 373 K. The ΔT values for the 4 cm and 5 cm apertures are similar, while those for the 10.8 cm aperture show significant increases in the absolute value of ΔT.

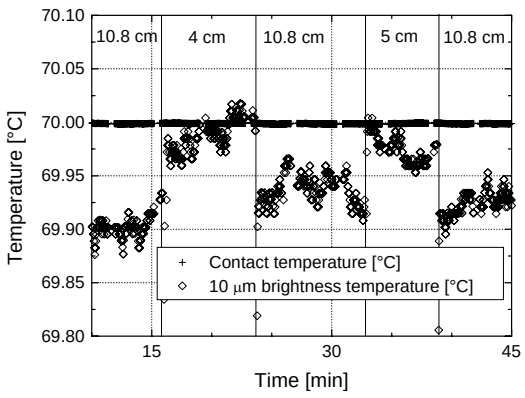

Figure 1: TXR measurement of the WBBB at 70 ºC.

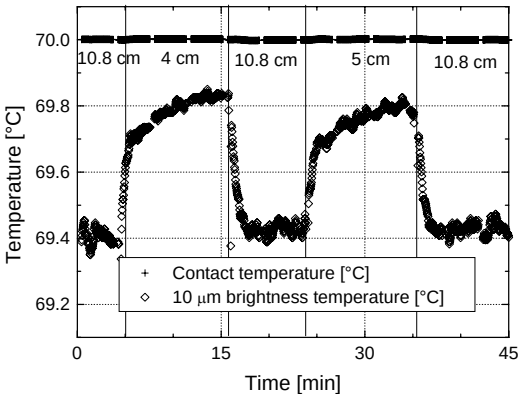

Figure 2: TXR measurement of the OBBB at 70 ºC.

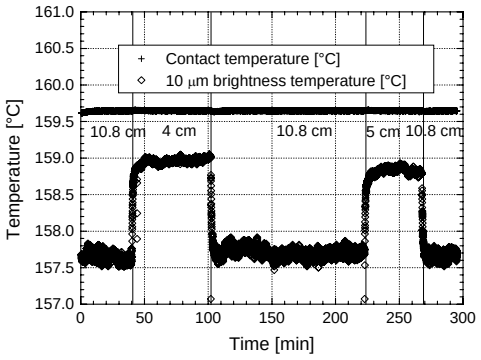

Figure 3: TXR measurement of the OBBB at160 ºC.

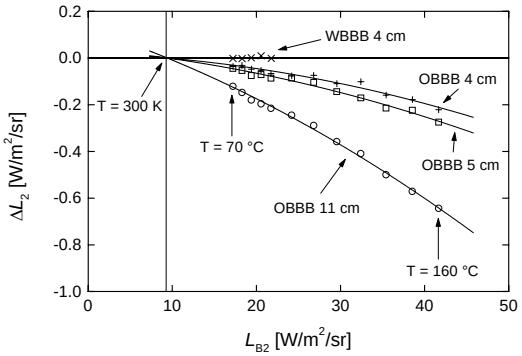

Figure 4: ΔL versus L_{B2} for OBBB.

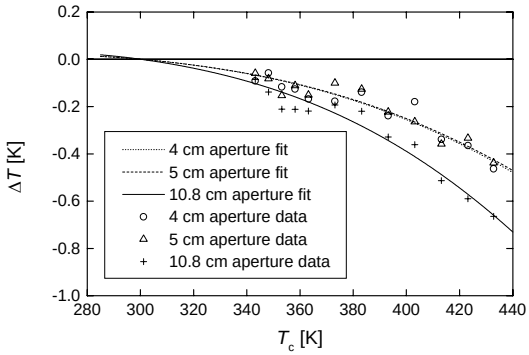

Figure 5: ΔT versus T_c for OBBB (estimate of uncertainty is 0.06 K, Type B, k=1).

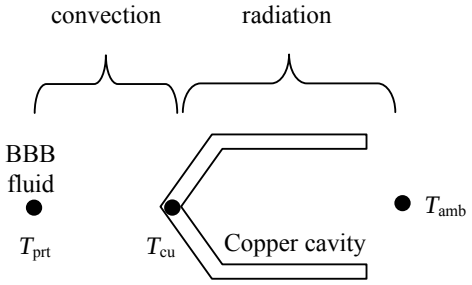

Figure 6: 1-D heat transfer model for comparison of WBBB and OBBB.

7. HEAT TRANSFER MODELING

A 1-D heat transfer model,

$$h \cdot \left(T_c - T_{cu}\right) = \varepsilon \cdot \sigma \cdot \left(T_{cu}^4 - T_{amb}^4\right), \tag{12}$$

treats the balance between convection and the radiation processes in Fig. 6. The Stefan-Boltzmann constant [7] is $\sigma = 5.6704 \times 10^{-8}$ W/m^2/K^4. Equation (12) assumes a negligible paint thickness and uniform fluid and cavity temperatures. The convection coefficient h was determined from the flowrate and temperature-dependent BBB fluid properties (density, kinematic viscosity, viscosity, thermal conductivity, and specific heat) [10, 11]. Using inputs ($T_{amb} = 298$ K, $T_c = 343$ K, $\lambda = 10$ μm, and $\varepsilon = 0.9997$), the results are shown in Table 3. From Fig. 5, the OBBB reading with the 10.8 cm aperture is less than that of the WBBB by about 85 mK, while Eq. (12) predicts that the OBBB temperature should be 178 mK less than the WBBB temperature. The higher value of T_{Cu} in the WBBB is mainly due to the lower water viscosity (μ in Table 3) and consequently a higher h value. This heat transfer model overpredicts the temperature discrepancy by about 93 mK but correctly reveals that T_{cu} in the OBBB should be lower that in the WBBB.

Table 3: Temperatures and parameters for comparison of WBBB and OBBB.

BBB Type	μ [N·s/m^2]	h [W/m^2/K]	T_{cu} [K]	$T_{cu,txr}$ [K]
WBBB	0.000389	23,381.3	342.986	343.150
OBBB	0.004000	1,749.7	342.808	343.065
OBBB – WBBB			-0.178	-0.085

8. CONCLUSIONS

The 1-D heat transfer model correctly predicted that the OBBB radiance temperature should be less than that of the WBBB but overpredicted the actual temperature discrepancy. The discrepancy between the WBBB and the OBBB can be explained by the different heat transfer properties of the two fluids. That is, the lower viscosity of water results in a higher convection heat transfer coefficient and consequently a higher copper temperature T_{cu}. Better heat transfer modeling can be produced by investigating aperture and temperature effects and by employing a 3-D model.

TXR data readily allows for the calculation of ε and ΔT. The TXR properly calibrated with the WBBB in the temperature range from 70 ºC to 90 ºC can be used to correct for calibration offsets at higher temperatures on the OBBB from 100 ºC to 160 ºC. The total offset, read from Figs. 2 and 3, is the sum of two contributions. The first accounts for thermal effects and is the temperature offset directly read from Fig. 5. The second accounts for optical effects due to a non-unity emissivity as listed in Table 2. For example, at 70 ºC the discrepancy due to thermal effects is about 0.1 ºC, while that due to optical effects is about 0.5 ºC. At 160 ºC, the discrepancies due to thermal and optical effects are 0.65 ºC and 1.35 ºC, respectively. The TXR model in Eq. (5) can be readily applied with other blackbody sources resulting in reduced uncertainties.

REFERENCES

[1] Fowler, J.B., "A Third Generation Water Bath Based Blackbody Source," *Journal of Research of the National Institute of Standards and Technology* **100**, 591-599 (1995).

[2] Fowler, J.B., "An Oil-Bath-Based 293 K to 473 K Blackbody Source," *Journal of Research of the National Institute of Standards and Technology* **101**, 629-637 (1996).

[3] Rice, J. P., and Johnson, B. C., "The NIST EOS thermal-infrared transfer radiometer," *Metrologia* **35**, 505-509 (1998).

[4] Rice, J. P., Bender, S. C., and Atkins, W. H., "Thermal-infrared scale verifications at 10 micrometers using the NIST EOS TXR," *SPIE*, **4135**, 96-107 (2000).

[5] Rice, J. P., "TXR interface requirements document," Version 2.2 (2001)

[6] Rice, J. P., Bender, S. C., Atkins, W. H., and Lovas, F. J., **"**Deployment test of the NIST EOS thermal-infrared transfer radiometer," *Int. J. Remote Sensing* **24**, 367-388 (2003)

[7] P. J. Mohr and B. N. Taylor, "The 2002 CODATA Recommended Values of the Fundamental Physical Constants, Web Version 4.0," available at physics.nist.gov/constants (National Institute of Standards and Technology, Gaithersburg, MD 20899, 9 December 2003).

[8] Rice, J.P., et al., "Calibration of the NIST thermal-infrared transfer radiometer against a cryogenic blackbody," in preparation, 2003

[9] Rice, J.P., et al., "The Miami2001 Infrared Radiometer Calibration and Intercomparison. Part I: Laboratory Characterization of Blackbody Targets," *Journal of Atmospheric and Oceanic Technology*, **21**, 258-267 (2004).

[10] Incropera, F.P., and DeWitt, D.P., "Fundamentals of Heat and Mass Transfer," John Wiley & Sons, New York, 2002

[11] Hart Scientific, Inc., personal communication (2002).

Addresses of the Authors:

Benjamin K. Tsai, Optical Technology Division, 100 Bureau Drive Stop 8441, Gaithersburg, MD 20882-8441, USA, tel. +1 301 975 2347, fax +1 301 869 5700, e-mail: benjamin.tsai@nist.gov, website: http://physics.nist.gov/Divisions/Div844/div844.html.

Joseph P. Rice, Optical Technology Division, 100 Bureau Drive Stop 8443, Gaithersburg, MD 20882-8443, USA, tel. +1 301 975 2133, fax +1 301 869 5700, e-mail: joe.rice@nist.gov, website: http://physics.nist.gov/Divisions/Div844/div844.html.